This is a preprint submitted to Geomechanics for Energy and the Environment

Fusing physics-based and data-driven models to forecast and mitigate landslide collapse

Carolina Seguí,[1*] Manolis Veveakis[2*]

[1]Institute of Geomechanics and Underground Technology, RWTH Aachen University, Mies-van-der-Rohe-Str. 1, Aachen, 52074, Germany
[2]Civil and Environmental Engineering Department, Duke University, 100 Science Dr., 121 Hudson Hall, Durham, NC 27708, USA

*Carolina Seguí; E-mail: segui@gut.rwth-aachen.de
*Manolis Veveakis; Email: manolis.veveakis@duke.edu

Deep-seated landslides represent one of the most devastating natural hazards on earth, typically creeping at inappreciable velocities over several years before suddenly collapsing with catastrophic speeds. They can have detrimental consequences to society, causing fatalities and prone to affect transportation infrastructures. In this study, we validate that monitoring the basal temperature of a creeping landslide, and fusing it with physics-based modeling, can offer predictive and control capabilities for the landslide's response. The study shows that physics-based models can be trained in the same phase-space, and has been applied to four case studies for its validity. We anticipate our results to be the starting point for a new era in monitoring, controlling, and forecasting deep-seated landslides, aiming at alleviating their devastating impact on society.

Deep-seated landslides are sizeable slides involving millions of cubic meters of soil moving as a rigid block on top of a deep (below the roots of the trees and the groundwater level) basal layer of heavily deformed minerals. These landslides shear as translational/rotational (depending on the stratigraphy of the area), with very low velocities (cm/year) during long periods (years to tens of years). However, their collapse is usually very sudden, happening within minutes and without previous warning (*1, 2*), reaching high velocities, as high as the $120m/s$ reported at the 1963 Vaiont landslide in Italy (*3*). The catastrophic and fast collapse of this kind of landslides makes the evacuation of the area that could be affected almost impossible, thereby possibly causing fatalities and infrastructure damages (*3–7*). Moreover, the lack of understanding of the physical processes behind the mechanisms of failure of this kind of landslides makes the development of reliable, data-driven, early warning systems (or tools/protocols to stop the acceleration of the landslide) challenging, therefore potentially causing significant damages to civil infrastructures. As shown in Fig. 1A, the landslide-prone areas spread worldwide, having a detrimental fatality rate (Fig. 1B). This figure highlights that landslides are a globally threatening natural hazard with incommensurate consequences.

A notable example of disproportionate consequences is the case of the 1963 Vaiont landslide in Northeastern Italy, which is among the top human-related catastrophes in history (*8*), with almost 2000 fatalities and unprecedented infrastructure damage (*3*). Since the landslide collapsed in 1963, several studies have presented different mechanisms involved as triggering factors of the acceleration and final collapse of deep-seated landslides. Some models tried to forward predict the catastrophic collapse of a landslide by, for example, inverting the field velocity data until it reaches zero or its displacement goes to infinity (*2, 9, 10*). However, these models are predominantly phenomenological and data-driven, thus not accounting for additional information considered the key to the problem. Such physics-based input includes the characterization and response of the material deforming inside the sliding surface (shear band), being the most critical part of a deep-seated landslide, and where all the physical-mechanical processes that determine the evolution of the landslide are operating (*11*). Hence, it is imperative to seek more answers on the behavior of a deep-seated landslide by attempting to enrich our data-driven capabilities with physics-based constraints stemming from the response of the shear band material to external loading (*12–20*).

It has been seen in monitored landslides that external factors, such as the variations of groundwater, trigger the movement of the landslide (*21–23*). These groundwater variations usually depend on seasonal/heavy rainfall (such as the Mud Creek landslide), snow melting (such as the El Forn landslide), or a nearby dam (such as the Vaiont and Shuping landslides). Moreover, other studies (*20*) show that adding internal factors in the model of a deep-seated landslide, such as material properties of the shear band, constrain triggering factors of the behavior of a deep-seated landslide and follow its accelerations during its creeping phase until its final collapse. Most deep-seated landslides present a shear band formed by clay or clay-like materials, which can be thermal and velocity-sensitive (*24, 25*) when the material experiences changes in pressure and is sheared, thus facilitating the acceleration of the landslide.

The difficulty of adding too much information from the physical mechanisms operating in the landslide's shear band is how to evaluate these parameters in the unavailability to access shear band material. For this reason, we suggest a method of fusing a physics-based model with data-driven parameter constrain by using an energy-based mathematical model in a reduced and dimensionless form (that depends on a single dimensionless parameter that can be constrained by the data) (*20, 25*). The model is described in the Supplementary Materials (Methods) and includes a single dimensionless parameter, the Gruntfest number (*26*) Gr, expressing the ratio of the mechanical work converted into heat over the heat diffusion capabilities of the shear-band material (Eq. S1). The Gruntfest number includes all the material properties at hand (thermal conductivity, rate and thermal sensitivities, and reference rate) (*24*), as well as the thickness of the shear band and the loading shear stress (applied on the shear band from the external loading sources, such as gravity and groundwater) (*20, 25*). In the absence of detailed information on the material, this dimensionless parameter can be used as a free parameter and be constrained by available data (*25*).

By therefore studying the stability of the heat energy-based equation (Eq. S3), we obtain a phase-space of the model by plotting the Gruntfest number against the basal temperature (see Methods section). This phase-space is delimited by a black line in Fig. S1A and indicates the area of stability of the landslide. While the basal temperature and Gruntfest remain within the stable area of the phase-space (grey area of Fig. S1A), the landslide remains in a stable creeping regime and reacts to any changes in the loading stresses or basal temperature. As soon as the basal temperature and Gruntfest transition to the unstable area of the phase-space (white area of Fig. S1A), the landslide becomes unstable and accelerates catastrophically, without any response to remediation actions (*20*). The physics of the model are, therefore, giving critical values of temperature and loading stress (i.e., Gruntfest). These results allow us to forecast when the landslide will turn unstable and collapse catastrophically, as long as the ”typically unobservable” fields of (dimensionless) basal temperature and shear stress can be measured or inferred by the observable quantities of the collected data (typically displacement/velocity and groundwater pore pressure).

In this study, we test the applicability of the aforementioned physics-based model (*20*) on data from four deep-seated landslides: the Vaiont landslide (in Italy) (*20*) and the Mud Creek landslide, both of which collapsed catastrophically after prolonged creeping phases; the currently active Shuping landslide (in the Three Gorges Dam, China); and the El Forn landslide (Andorra) (*25*). We first showcase the validity of the theoretical phase-space by presenting the results of monitoring the temperature of an active deep-seated landslide (*25*). The El Forn landslide was instrumented with a thermometer in the shear band, and four months of recording data are shown in Fig. S2A (Supplementary Materials), along with the groundwater pressure (*25*).

The data show that the thermal response of the shear band directly depends on the water pressure. By using the monitored temperature and pore pressure in the model, we can calculate temperature in our model from Eq. S3 and reproduce the field temperature by tuning the base value of the Gruntfest number (Eq. S5). Having constrained the single parameter of the model, we can now forecast the velocity/displacement of the landslide from Eq. S3, as shown in Fig. S2B. Finally, once the data have been used to calibrate the model, we can map the temperature/normalized velocity and the Gruntfest/shear stress/(pore) pressure data of the landslide on the phase-space of the model (see Methods section), as shown in Fig. S2C. We observe that the field data (temperature and pore pressure/shear stress) and the calculated data as Gruntfest and velocity follow the phase space suggested by the model. In a recent paper (*25*), the authors obtained the input parameters of the model for this landslide from laboratory experiments on the shear band's material, confirming the validity of the inverted values of the Gruntfest number.

Having validated the feasibility of the physics-based model through monitoring the basal temperature of an active landslide (*20*) (Fig. S2), we will explore in the next steps if the physics-based model can be equally used without having detailed information about the basal temperature and the material's parameters. To this end, we will apply the model at the Mud Creek landslide, which catastrophically collapsed on May 20th of 2017, after years of creeping (*27*). The only available data are the velocity obtained from satellite imaging of the area and the normalized pore pressure inferred from the precipitation data (*27*) (Fig. 2A). Using the pore pressure as the driving loading factor (see Methods section) and calibrating the value of the Gruntfest number required for the model to follow the phase-space, we retrieve that the landslide collapses during the last decrease of the pore pressure. Fig. 2A shows the data of the pore pressure and the velocity, with the forecasted velocity from our model. In Fig. 2B, we show that by using the velocity and pore pressure data (shear stress) and calibrating the physics-based model on its phase-space, we can adequately reproduce the history of the Mud-

Creek slide without any knowledge of the basal material. The results of the field and calculated data of the Mud Creek landslide follow the stable area of the phase-space (lower branch of the steady-state curve) until the (pore) pressure/Gruntfest and velocity/basal temperature reach the stable threshold, therefore entering the tertiary creep of the landslide and its catastrophic collapse.

Moreover, the model is applied to the Shuping and Vaiont landslides (*20*). These two landslides have the same characteristics of the shape of the slide and the material of the shear band (clays) and are ancient landslides reactivated upon the construction of a dam in their vicinity. Thus, both landslides' behavior depends directly on the pore pressure variations caused by the dam's operations. The Vaiont landslide collapsed catastrophically (Fig. 3B) while the Shuping landslide remains actively creeping (Fig. 3C). The results of the transient model applied to the two case studies show that, indeed, the model can be trained on its phase-space and be used to forecast the evolution and stability of the landslide (Fig. 3A), without deep knowledge of the material's properties.

Summarizing the importance of the phase-space in landslide forecasting and control, Fig. 3A shows the response of all landslides in the observed velocity-pressure phase-space calculated from the unobserved temperature-Gruntfest number phase-space. Fig. 3A suggests that regardless of the size and characteristics of each landslide and its shear band material, all landslides can be mapped in the same phase-space, whether they remain active or already collapsed. These results suggest that the temperature is a key factor of the behavior of a deep-seated landslide. Adding the basal temperature in the model to forecast a landslide behavior has been previously discussed and proved by the authors (*25*). Thus, monitoring the temperature in the shear band of the landslide and implementing the presented model in real-time allows us to forecast and control the behavior of the landslide, even with limited knowledge of the shear band's material. This new model, thus, allows the engineers in charge to take remediation measures while the landslide is stable and prevents catastrophic acceleration.

References and Notes

References

1. I. J. Smalley, *Nature* **272**, 654 (1978).

2. B. Voight, *Nature* **332**, 125 (1988).

3. L. Mueller, *Felsmech. Ingenieurgeol.* **2**, 148 (1964).

4. G. Preisig, *Q. J. Eng. Geol. Hydrogeol.* **52**, 326 (2019).

5. K.-J. Chang, A. Taboada, *J. Geophys. Res. Earth Surf.* **114** (2009).

6. C. Huang, M. Chen, M. Hsu, *Terr. Atmospheric Ocean. Sci.* **T13**, 387 (2002).

7. W. Wang, M. Chigira, T. Furuya, *Engin. Geol.* **69**, 1 (2003).

8. International year of planet earth - global launch event 12-13 february 2008 (2008).

9. M. Saito, *Proc. 6th Int. Conf. on Soil Mechanics and Foundation Engineering, Montreal* (1965), vol. 1, pp. 537–541.

10. M. Saito, *Proc. 7th Int. Conf. on Soil Mechanics and Foundation Engineering, Mexico* (1965), vol. 2, pp. 419–445.

11. F. M. Gonzalez de Vallejo, Luis I., *Geological engineering* (CRC Press/Balkema, Leiden, The Netherlands, 2011).

12. I. Vardoulakis, *Mech. Cohesive Frict. Mater.* **5**, 443 (2000).

13. I. Vardoulakis, *Geotechnique* **52**, 157 (2002).

14. K. Chang, A. Taboada, M. Lin, R. Chen, *Engin. Geol.* **80**, 151 (2005a).

15. E. Veveakis, I. Vardoulakis, G. DiToro., *J. Geophys. Res.* **112**, F03026 (2007).

16. L. Goren, E. Aharonov, *Geophys. Res. Lett.* **34**, L07301 (2007).

17. K. Regenauer-Lieb, D. Yuen, F. Fusseis, *Pure. Appl. Geophys,* **166**, 1885 (2009).

18. L. Goren, E. Aharonov, M. H. Anders, *J. Geophys. Res.* **115**, B10210 (2010).

19. F. Cecinato, A. Zervos, E. Veveakis, *Int. J. Numer. Anal. Methods Geomech.* **35**, 1507 (2011).

20. C. Seguí, H. Rattez, M. Veveakis, *J. Geophys. Res. Earth Surf.* **n/a**, e2019JF005203. E2019JF005203 2019JF005203.

21. K. Terzaghi, *Application of Geology to Engineering Practice* (Geological Society of America, 1950), pp. 83–123.

22. K. Terzaghi, *Theoretical soil mechanics* (John Wiley and Sons, New York, 1943).

23. R. M. Iverson, J. J. Major **99**, 579 (1987).

24. I. Vardoulakis, *Int. J. Solids Struct.* **39**, 3831 (2002).

25. C. Seguí, M. Veveakis, *Landslides* **18**, 3953 (2021).

26. I. Gruntfest, *Trans. Soc. Rheol.* **7**, 95 (1963).

27. A. L. Handwerger, M.-H. Huang, E. J. Fielding, A. M. Booth, R. Bürgmann, *Scientific Reports* **9**, 1569 (2019).

28. S. T. Juang CS, K. DB, *PLOS ONE* **14**, e0218657 (2019).

29. D. Kirschbaum, T. Stanley, Y. Zhou, *Geomorphology* **249**, 4 (2015). Geohazard Databases: Concepts, Development, Applications.

30. A. R. H. Y. H. S. Kirschbaum, D.B., A. Lerner-Lam, *Natural Hazards* **52**, 561 (2010).

31. J. R. Rice, *J. Geophys. Res.* **111**, B05311 (2006).

Acknowledgments

The authors would like to acknowledge Xavier Planas from the Government of Andorra to provide us the core samples of the landslide and the field data and Jose Moya from BarcelonaTech University to provide us the field data. This work was supported by the NSF CMMI-2006150 project. Both authors contributed equally in all aspects of this work. he authors declare that they have no competing financial interests. Correspondence and requests for materials should be addressed to both authors (CS email: segui@gut.rwth-aachen.de, MV email: manolis.veveakis@duke.edu).

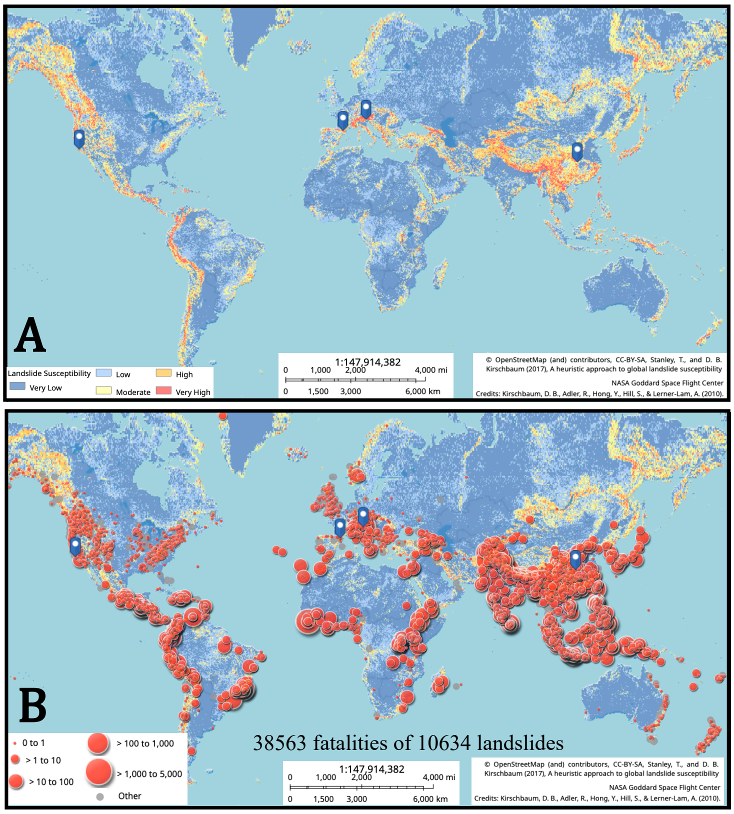

Fig. 1. Global impact of landslides. (**A**) World map of landslide susceptibility, highlighting areas prone to landslides with red. The four pins correspond to the locations of the four deep-seated landslides discussed in this work. (**B**) Map of fatalities from landslides worldwide between 1956-2020 (last access July 2020). The data for this figure was collected from NASA's Cooperative Open Online Landslide Repository (COOLR) (*28–30*). Highlighted in blue the four case studies that we present in this study: the El Forn landslide (Andorra), the Vaiont landslide (Italy), the Shuping landslide (Three Gorges Dam, China), and the Mud Creek landslide (California, USA).

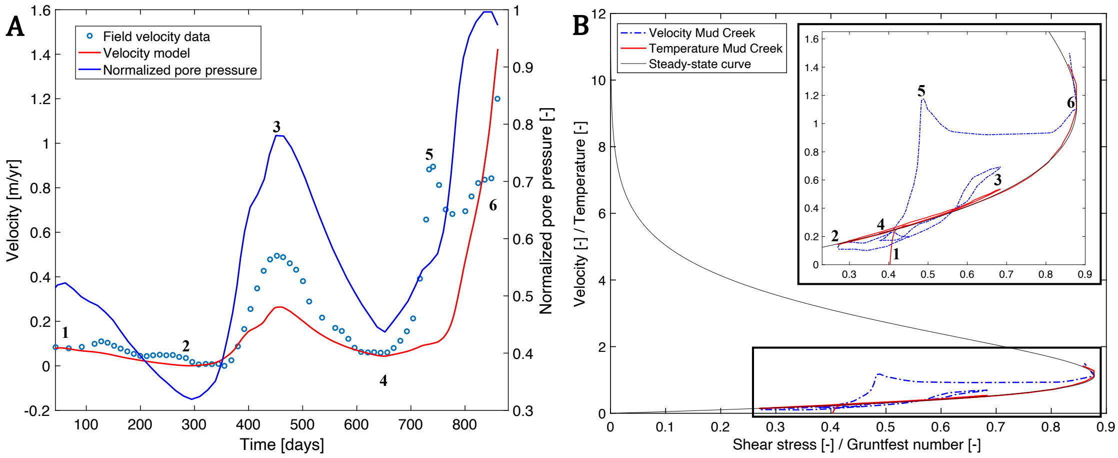

Fig. 2. Forecasting and controlling the response of the Mud Creek landslide. (**A**) Pore pressure (blue line) and velocity data (blue dots) from (*27*), with the velocity calculated in our model (red line). (**B**) Basal temperature and Gruntfest number calculated in our model mapped in the phase-space, as well as the field velocity and pore pressure (shear stress). The inset shows a zoom of the field and calculated data behavior in the phase space with numbers correlating the data shown in Fig. 2A, showing the point of when the landslide turns unstable and collapses catastrophically.

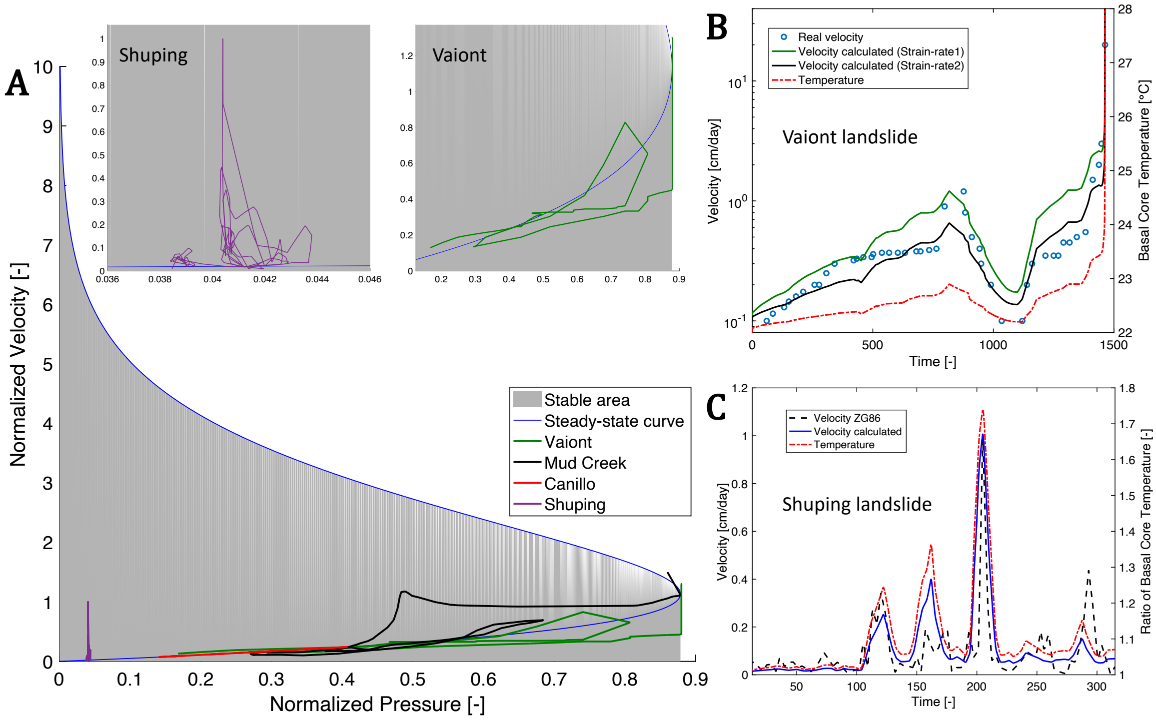

Fig. 3. Controlling deep-seated landslides through basal temperature. (**A**) Mapping of the calculated loading pressures and velocities of the four landslides on the phase-space of the model's response. We observe that all four landslides follow the model's phase-space, with the Vaiont and the Mud Creek collapsing catastrophically when exceeding the stable (gray) area of the model, and the El Forn and Shuping inside the stable area of the phase-space. It is therefore suggested that deep-seated landslides can be controlled by maintaining their pressure and temperature inside the grey area of this phase space. The insets show a zoom of the Shuping and Vaiont landslides in the phase-space. (**B**) The Vaiont landslide field velocity with the calculated velocities and basal temperature. As the velocity and temperature behavior show, once the phase-space (Fig. 3A) is exceeded, both variables (velocity and temperature) increase infinitely, thus, a catastrophic collapse occurs. (**C**) The Shuping landslide field velocity, with the calculated velocity and basal temperature. It is shown in Fig. 3A, that this landslide is still very

stable, regardless of the variations of groundwater pressure and temperature experienced until the end of this data period.